Industrial Crops & Products 240 (2026) 122638

Contents lists available at ScienceDirect

Industrial Crops & Products

journal homepage: www.elsevier.com/locate/indcrop

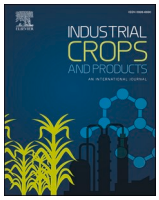

Optimizing rubberwood performance through rapid heated platen thermal modification: A sustainable approach for enhanced dimensional stability, decay resistance, and mechanical integrity

Zhipeng Zhu [a], Jingyao Zhao [a], Xiaoxue Song [a], Qiaofang Zhou [b], Xiangyu Zhao [b], Wanli Cheng [a,*], Antoni Sánchez-Ferrer [c,*], Dengyun Tu [b,*]

[a] Key laboratory of Bio-based Material Science and Technology of Ministry of Education, Northeast Forestry University, Harbin 150040, China
[b] Key Laboratory of Bio-based Materials and Energy, Ministry of Education, South China Agricultural University, Guangzhou 510642, China
[c] Wood Materials Science, Wood Research Institute of Munich (HFM), TUM School of Engineering and Design, Technical University of Munich, Winzererstrasse 45, Munich 80797, Germany

ARTICLE INFO

Keywords:
Rubberwood
Thermal modification
Heated platen method
Chemical composition
Mechanical properties
Non-destructive assessment

ABSTRACT

The global shift toward sustainable development has increased the demand for renewable biomass materials, with rubberwood emerging as a promising resource due to its rapid growth and potential for carbon sequestration. However, its susceptibility to dimensional instability and decay has significantly hindered its widespread industrial application. While current solutions address certain challenges, they often come with disadvantages such as high costs, inefficiencies, and/or environmental risks. This study introduces an innovative heated platen modification method designed to overcome these limitations. By employing direct-contact heating, a rapid surface modification is achieved between 5 and 15 min at temperatures ranging from 250 to 290 ℃. It creates a functionally graded material structure that enhances surface properties while maintaining core strength. Compared to untreated materials, the treated specimens exhibited a 524 kg/m^3 increase in surface density, a 29–47 % reduction in modulus of rupture, a 2–11 % decrease in modulus of elasticity, a 2–31 % drop in screw holding power, a 33 % reduction in shrinkage, and a 58 % decrease in swelling. Surface natural decay resistance performance improved significantly, with a 39–45 % decrease in mass loss rate. Mechanistic analysis revealed that selective hemicellulose degradation and lignin redistribution enhanced the overall degree of crystallinity from 40 % to 64 % without compromising the crystalline domains, collectively improved dimensional stability and decay resistance without severe strength compromise. A key contribution of this study is establishing quantitative correlations between color parameters and performance metrics, revealing strong relationships between ΔE^* and mechanical properties, chemical composition, and dimensional stability, and suggesting the chromatic indices as viable proxies for performance evaluation. However, predicting fungal durability via color requires further study due to decay mechanism complexities. This work advances the sustainable utilization of plantation species by integrating controlled surface modification, performance enhancement, and non-destructive assessment, offering a paradigm for efficient wood processing aligned with circular economy principles.

1. Introduction

The global push toward sustainable development has increasingly emphasized the utilization of renewable biomass materials as a key strategy for mitigating carbon emissions and combating climate change. Wood is recognized as one of the world's most versatile and sustainable biopolymer composites (Friend et al., 2022; Huang et al., 2025; Rahiminejad et al., 2024; Zouari et al., 2024). As the largest producer and consumer of wood products, China has set an ambitious "peaking carbon dioxide emissions by 2030 and carbon neutrality by 2060" as the national objective, which requires the adoption of more eco-friendly materials and energy-efficient processing technologies. In this context, the wood industry is undergoing a profound transition toward green and low-carbon development (Mi et al., 2020; Yue et al., 2023). At the same

* Corresponding authors.
E-mail addresses: nefucwl@nefu.edu.cn (W. Cheng), sanchez@hfm.tum.de (A. Sánchez-Ferrer), tudengyun@scau.edu.cn (D. Tu).

https://doi.org/10.1016/j.indcrop.2026.122638
Received 11 August 2025; Received in revised form 20 November 2025; Accepted 2 January 2026
Available online 6 January 2026

time, with growing global ecological awareness, many countries have implemented stringent policies and measures to protect valuable timber resources. These initiatives have further exacerbated the conflict between increasing wood demand and limited supply (Zhu et al., 2024a).

To address these challenges, several solutions have been proposed, including expanding fast-growing plantation areas, reducing wood waste during processing, maximizing utilization efficiency, increasing the recycling and utilization of waste wood, and enhancing wood protection and modification to extend service life (Huang et al., 2020; Zhu et al., 2024b). These measures represent crucial strategies for reducing carbon emissions and balancing supply and demand. Rubberwood (*Hevea brasiliensis*), a byproduct of latex production, has emerged as a promising biomass resource due to its rapid growth cycle, widespread availability, and carbon sequestration potential. However, its high nutrient content - approximately 8 % starch and free sugars - makes it susceptible to fungal decay, while its low natural durability and poor dimensional stability limit its widespread use in high-value industries such as furniture, flooring, and construction (Zhao et al., 2021; Zhu et al., 2021). Overcoming these challenges through innovative modification technologies is essential to unlocking the full potential of rubberwood as a sustainable alternative to traditional, carbon-intensive building materials. Conventional methods, such as chemical preservatives, have been widely used but raise environmental and health concerns due to their toxicity and non-biodegradability (Yao et al., 2023; Zhao, S. et al., 2024a). In contrast, thermal modification has gained popularity as an eco-friendly alternative, as it relies solely on heat to induce physicochemical changes in the wood's structure without the use of harmful chemicals (Haseli et al., 2024; Xiang et al., 2024).

Thermal modification has been shown to be an effective method for improving wood properties, such as dimensional stability and resistance to biodegradation (Ditommaso et al., 2020). However, thermally modified wood often experiences significant degradation in mechanical properties, volume loss, mass and chemical changes (Xia et al., 2025). Moreover, the conventional thermal modification process is complex, typically requiring treatment durations exceeding 10 h, resulting in high energy consumption. The need for specialized reactors, such as steam or vacuum chambers, further increases both capital and operational costs. According to Borrega and Kärenlampi, the mechanical properties of wood, including strength, fracture strain, and toughness, deteriorate with thermal treatment, with degradation correlating to mass loss caused by the autocatalytic decomposition of cell wall components (Borrega and Kärenlampi, 2007). Esteves *et al.* observed that mass loss in pine and eucalyptus increased with prolonged treatment duration and elevated temperatures, while the modulus of elasticity and bending strength generally decreased correspondingly. These alterations make thermally modified wood unsuitable for structural applications that require high strength-to-mass ratios (Esteves et al., 2006). Although Yue *et al.* suggested that maintaining treatment temperatures within the 170–180 ℃ range could preserve sufficient strength for structural applications, the dimensional stability of the material cannot be guaranteed under these conditions (Yue et al., 2023). He *et al.* found that treating elmwood with tung oil at 210 ℃ could reduce volumetric shrinkage by 85 %, whereas the process still required more than 6 h of treatment (He et al., 2022). These limitations highlight the need for a more efficient and targeted modification approach.

This study presents an innovative heated platen treatment thermal modification method specifically designed to address these critical limitations. Thermal surface modification through direct-contact heating significantly reduces processing time (5–15 min compared to the conventional 8–24 h). The aims are to optimize the trade-off between improved dimensional stability and minimal strength reduction. This research also systematically investigates the fundamental relationships between chemical structure, chemical composition, microstructure, physical properties, mechanical properties, natural decay resistance and visual characteristics in modified rubberwood. We establish quantitative correlations between surface color parameters and key performance indicators (dimensional stability, decay resistance, and mechanical strength) to develop a non-destructive quality assessment framework, enabling rapid quality evaluation in industrial settings. Moreover, the energy-efficient nature of the heated platen method aligns with circular economy principles by minimizing waste and reducing the carbon footprint of wood processing.

2. Materials and methods

2.1. Materials

The samples used in this study were rubberwood (*Hevea brasiliensis*) obtained from Thailand. The dimension of the sawn timber was 1000 × 110 × 23 mm^3 (L×T × R), with an air-dried density of 650–700 kg/m^3 and 12–15 % initial moisture content. The samples were exclusively sourced from rubber trees cultivated in proximal regions within the same forest plantation, and the sampling process was randomized. The samples were prepared by selecting flatsawn lumbers without visible defects, measuring 300 × 15 × 21 mm^3 (L×T × R). All specimens were stored for subsequent treatment under controlled conditions at 20 ℃ and 65 % RH for one month, resulting in a moisture content of around 12 %.

2.2. Preparation of modified rubberwood

The preparation process used a laboratory-scale single-opening hot press (XLB-0.6 ×0.6 m^3, JinJiuzhou, China), equipped with an electric heating and a cooling water system. The samples underwent a simplified two-stage heating and cooling process. Therefore, the modification process in this study was carried out using a simple and efficient procedure, requiring only a relatively brief duration. Firstly, the upper and lower plate temperatures were adjusted to the desired level and stabilized. The samples were placed on the lower heated platen with 20 mm thickness gauges on both sides to ensure close contact. Subsequently, the samples were radially compressed at 5 MPa and a rate of 0.5 mm/s. Timing commenced upon contact of the heated platen with the thickness gauge, initiating the specified treatment duration under constant 5 MPa pressure. Upon completion of this period, the heated platen was opened, and the sample was transferred to cool down at room temperature. Two flatsawn lumbers were processed each time, and a specific area was designated before processing to track the changes in surface performance. After thermal modification, all specimens were conditioned for one month at 20 ℃/65 %-RH. Combinations of different treatments produced 9 specimens and an untreated specimen, each with a different treatment: three heat treatment temperatures were studied, *i.e.*, 250, 270 and 290 ℃, at three different heating durations of 5, 10 and 15 min.

2.3. FTIR characterization, XRD structural analysis and chemical analysis composition

For the FTIR characterization and the chemical analysis composition, the material was ground into powder within 1 mm of the surface before analysis, as this 1 mm area was guaranteed to have undergone heat treatment. The control and treated samples were characterized by FTIR using a Fourier transform infrared spectrophotometer (SPECTRUM100, PerkinElmer Inc., USA), and before FTIR characterization, samples were milled, sieved through the 80 mesh screen, and oven-dried at 103 ℃. FTIR spectra were recorded by combining 16 scans over the wavenumber range of 600–4000 cm^{-1} with a 4 cm^{-1} resolution.

The wood structure was analyzed by X-ray diffractometry (AB 250Xi, Thermo Fisher Scientific Inc., USA) with $\lambda_{CuK\alpha}$ radiation of 0.15178 nm. The sample size used for WAXS analysis was a 10 × 10 × 2 mm^3 (T × L × R) sheet. WAXS scattering intensity profiles were collected using 40 kV and 30 mA CuKα radiation. The X-rays were directed parallel to the wood fibers, and the scan was conducted at a scanning rate of 10°/min within the 5° to 85° (2θ) range, which corresponds to a scattering

wavevector of 3.5 $nm^{-1} < q < 55\ nm^{-1}$, where q is the scattering wave vector ($q = 4\pi\sin\theta/\lambda$). The degree of crystallinity (χ) was calculated by the deconvolution of the WAXS signal into crystalline and amorphous peaks in the WAXS patterns, the areas of which give the $\chi = A_{crystalline} / (A_{crystalline} + A_{amorphous})$ (Ahmed et al., 2025; Engelhardt et al., 2024).

The content of cellulose (CC), hemicellulose (HC), lignin (LC), and extractives (EC) of rubberwood was analyzed following the method outlined by the National Renewable Energy Laboratory (Sluiter et al., 2008). The acid-soluble lignin (ASL) was measured using a UV–vis spectrophotometer (Evolution 220, Thermo Fisher Scientific, Shanghai, China), with 4 % dilute sulfuric acid as the control. The glucose and xylose quantities after hydrolysis were measured using high-performance liquid chromatography, and these values were used to calculate the yields of cellulose and hemicellulose. Three replicates were used to determine the content of each component to verify the obtained results.

2.4. Microstructure characterization

After the cross section of the sample was trimmed by a sliding slicer (REM 710, Daiko Optical Machinery Co., Ltd, Japan), the surface morphology of the wood sample was observed by a scanning electron microscopy (SEM, EVO 18, Carl Zeiss, Germany) working with an accelerated voltage of 10 kV.

2.5. Physical properties

The drying shrinkage and swelling of the specimen in the tangential, radial, and volumetric directions, respectively, were measured according to the standard ISO 13061–13, 14, 15, 16 (2016). The weight and thickness of the specimen with a dimension of 20 × 20 × 20 mm^3 (L×T × R) were measured to an accuracy of 0.001 g and 0.001 mm, respectively. The tangential, radial and volumetric drying shrinkage rate of the specimen from waterlogged wood to air-dried wood - β_{wR}, β_{wT} and β_{wV}, respectively -, and the drying shrinkage rate from air-dried wood to absolute-dried wood - β_{maxR}, β_{maxT} and β_{maxV}, respectively - were calculated. The tangential, radial and volumetric thickness swelling rate of the specimen from air-dried wood to waterlogged wood - α_{wR}, α_{wT} and α_{wV}, respectively -, and the thickness swelling rate from absolute-dried wood to air-dried wood - α_{maxR}, α_{maxT} and α_{maxV}, respectively - were also calculated.

The density profile of the wood specimens was measured using an X-ray densitometer (DPX300-LTE, IMAL, Italy). Density measurements were recorded at 0.05 mm intervals throughout the thickness of the specimens with a dimension of 50 × 20 × 50 mm^3 (L × T × R) and measured along the thickness direction.

2.6. Mechanical properties

The mechanical properties of the wood specimens were determined using the universal testing machine (UTM5504, SUNS Company, Shenzhen, China). The screw holding power (SHP) test, surface hardness (the hardness of tangential, SH-T, and radial, SH-R, section), compressive strength parallel to grain (CS), modulus of rupture (MOR), and modulus of elasticity (MOE) were measured following the GB/T 17657 (2013), GB/T 1935 (2009), ISO 13061–12 (2017) and ISO 13061–3, 4 (2017) standards, respectively, with 10 replicates for each test. All specimens were conditioned in a humidity chamber maintained at 20 °C/65 %-RH until reaching a constant weight.

2.7. Determination of wood color

Wood color measurement was conducted on the samples using a portable spectrocolorimeter (CR10Plus, Konica Minolta, Inc., Japan). The color difference between the samples before and after treatment was expressed as ΔE^*, calculated using the CIE Lab method. In the experiment, each group consisted of 6 replicates measured 5 times. The physical images of the rubberwood surface were scanned using an Epson scanner V700 at a resolution of 1200 × 1200 dpi.

2.8. Surface natural decay resistance test

The natural decay resistance of wood was evaluated according to the GB/T 13942–1 (2009) with dimensions of 30 × 10 × 4 mm^3 (L × T × R). The surface of the sample, except for the heat-treated surface, was coated with epoxy resin. After the epoxy resin had fully cured, the sample was placed in a drying oven at 103 °C. The mass of the sample was recorded as m_0. After high-temperature sterilization, *i.e.*, 121 °C, the sample was placed in a medium containing white-rot fungi (*Coriolus versicolor* L. Quel.) and brown-rot fungi (*Gloeophyllum trabeum* Pers. Murrill). It was then cultured in an incubator at 85 % humidity and 28 ℃ for 12 weeks. After the culture period, the fungus attached to the sample surface was gently scraped off, and the sample was dried again in a drying oven at 103 ℃ until absolutely dry. The mass of the sample after drying was recorded as m_1. The mass loss rates of the samples after being corroded by white rot fungi (*MLW*) and brown rot fungi (*MLB*) were calculated according to GB/T 13942–1 (2009) standard. Each experimental group included 6 replicates.

2.9. Statistical analysis

To further evaluate the effects of treatment temperature and duration on various rubberwood properties, statistical analyses were performed using SPSS software. Significant differences between groups were assessed at a 95 % confidence level ($p < 0.05$), and linear regression analysis was conducted to investigate variable relationships.

3. Results and discussion

3.1. Chemical structure and chemical composition analysis

FTIR investigations were conducted to learn about the chemical changes in the samples upon thermal treatment. Fig. 1a shows the FTIR spectra for all samples treated at different temperature/duration conditions. The heat-treated samples showed changes in their chemical structure compared to the control sample, though the overall spectra remained similar (Fig. SI-1). Specifically, the most notable change was the degradation of hemicellulose during heat treatment, indicated by changes in the 1800–1535 cm^{-1} region, with a reduced peak intensity at 1735 cm^{-1} (C═O, stretching) an increased peak intensity at 1590 cm^{-1} (COO^-, stretching), and the appearance of several new peaks between 1735 and 1590 cm^{-1} of oxidized products from the degradation of hemicelluloses and other saccharide units. Additionally, the peak observed at 1230 cm^{-1} (C-O, stretching) showed an intensity decrease due to the removal of acetate groups as a result of the hemicelluloses degradation (Kavyashree and Krishna, 2012). Therefore, heat treatment modified several chemical structures of wood to some extent, and these differences in the degradation of cell wall components may be an important reason for the macroscopic performance changes of the rubberwood.

The WAXS analysis was performed in order to identify any change in the crystalline structure of the wood samples during the heat treatment process. The diffractograms of rubberwood samples before and after heat treatment were similar within the scattering range (Fig. 1b and Fig. SI-2). All samples showed the monoclinic crystalline structure with lattice parameters a = 7.9 Å, b = 8.0 Å, c = 10.2 Å, and g = 96.9° for the control sample corresponding to the cellulose I allomorph, and with small variations for the heat-treated samples (Table SI-1)

The degree of crystallinity of the control sample was 40 %, and as the treatment temperature and duration increased, the samples' degree of crystallinity increased between 50 % and 65 %, with a maximum value for the sample treated at 290 ℃ for 15 min. The hemicellulose

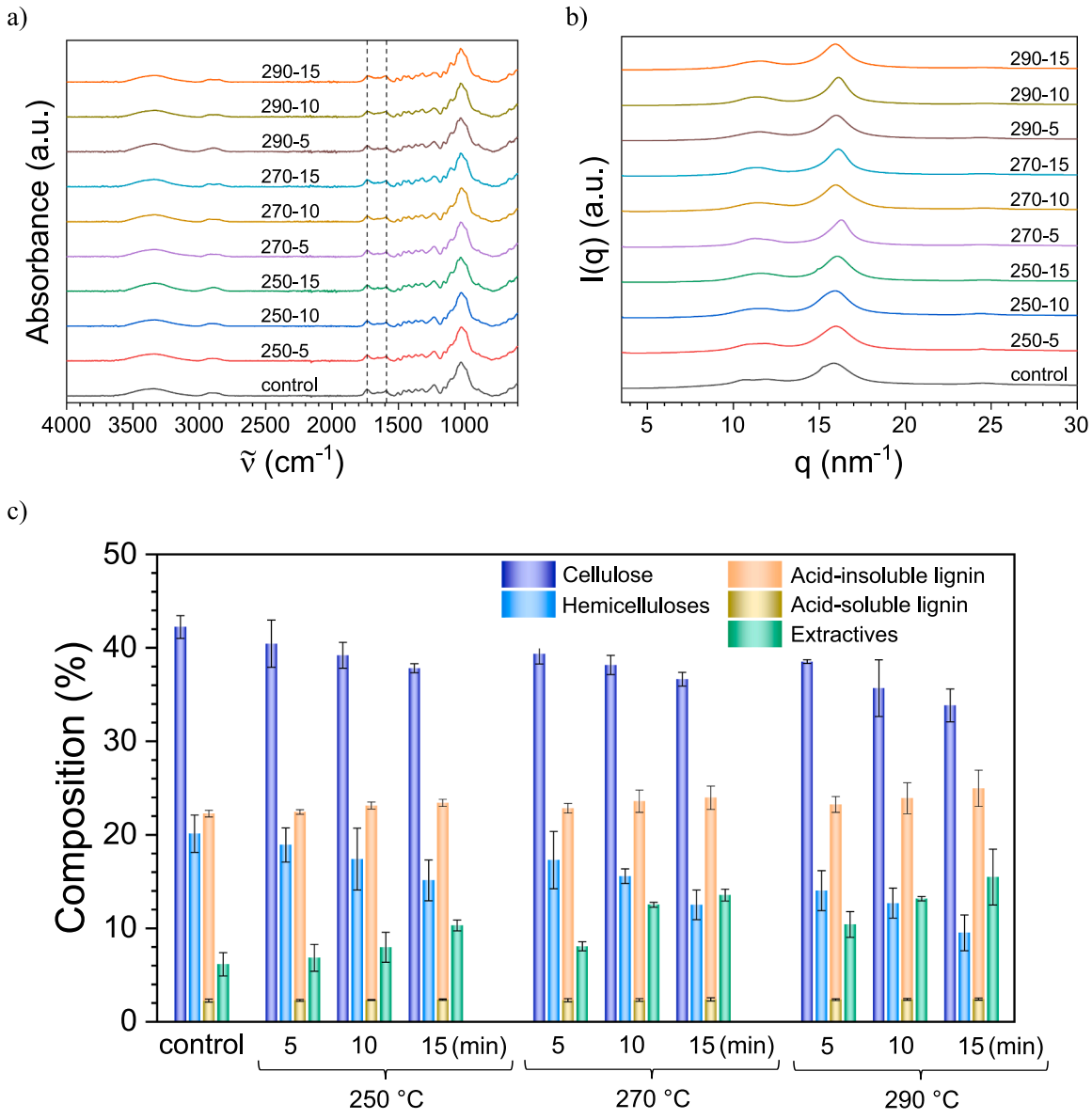

Fig. 1. a) FTIR spectra and b) XRD patterns for the heat-treated rubberwood samples and the control sample. c) Chemical composition of the heat-treated rubberwood samples and the control sample.

degradation causes a decrease in the amorphous content, resulting in an increase in the overall relative crystallinity of cellulose (Ahmed et al., 2025; Altgen et al., 2018; Sánchez-Ferrer et al., 2023). Interestingly, the crystallinity observed in this study was much higher than that in Chen's research (Chen et al., 2018). Although he treated rubberwood with superheated steam at temperatures ranging from 170 ℃ to 200 ℃. This discrepancy could be attributed to the distinctive treatment methodology used in this study, as the wood was processed by direct heating without requiring a medium. The immediate contact between the wood surface and the heating plate guaranteed optimal heat transfer efficiency. Furthermore, the heated platen method employed in this research demonstrated significantly greater operational simplicity compared to conventional heat treatment processes.

Chemical analysis was performed on all samples in order to identify which components degraded during the heat treatment process (Table SI-2). As shown in Fig. 1c, compared to the control sample, the relative content of amorphous cellulose and hemicelluloses gradually decreased as the treatment temperature and duration increased (Fig. SI-3). Specifically, the relative decrease in amorphous cellulose content at 250, 270 and 290 °C after 15 min was 10 %, 13 % and 20 %, respectively, while for hemicelluloses it was 25 %, 38 % and 53 % respectively, indicating that hemicelluloses decompose faster than amorphous cellulose. The changes in the relative contents of lignin and extractives in response to treatment temperature and duration differed from those of cellulose (Fig. SI-3). The relative increase in lignin content at 250, 270 and 290 °C after 15 min was 5 %, 8 % and 12 %, respectively, and for the extractives was 68 %, 121 % and 152 %, respectively. However, this increase was not due to a rise in the absolute amount of lignin, but rather because other components, such as hemicelluloses and amorphous cellulose, degraded more rapidly, thereby increasing the proportion of lignin in the remaining material. The increase in extractives content was especially pronounced and can be attributed to some degradation products from hemicelluloses and amorphous cellulose, which are detected as extractives afterwards and contribute to the final percentage of extractives (Candelier et al., 2013). The absolute percentage of degraded polysaccharides, *i.e.*, amorphous cellulose and hemicelluloses,

at the three different temperatures and after 15 min ot heat treatment was 9 %, 13 % and 19 %, whereas the absolute increase for the extractives together with the lignin content was 5 %, 9 % and 12 %, respectively, matching quite well the decrease of the formers with the decrease of the latter ones.

Therefore, the heating degradation sequence is the following: first, amorphous polysaccharides, *i.e.*, hemicelluloses and amorphous cellulose; then, partially the amorphous crosslinked lignin; and, finally, the crystalline cellulose. Under the treatment conditions in this study, the degradation of the three major components in the wood's surface layer was far greater than that observed in conventional low-oxygen heat treatment processes. The analysis of variance (ANOVA) results demonstrated that both treatment temperature and duration were highly significant ($P < 0.01$) and affected the content of cellulose, hemicelluloses, lignin and extractives. Moreover, treatment temperature exerted a more substantial influence on both the content of hemicelluloses and extractives, as evidenced by higher F-values. In contrast, the content of cellulose and lignin showed greater sensitivity to variations in treatment duration (Altgen et al., 2016; Windeisen et al., 2007).

3.2. Microstructure analysis

The heated platen treatment method significantly changed the microstructure of rubberwood, and these microscopic changes further influence the macroscopic properties. Fig. 2 illustrates the microstructure of the cross-sections of each heat treatment group at different magnifications. As shown in Fig. 2, at 250 ℃, the appearance of the wood rays was smooth and flat, with the integrity of the honeycomb structure largely intact. The fibers had relatively thick walls and were closely arranged, indicating that the wood's microstructure was not significantly damaged. The small granular starch in rubberwood maintained an ellipsoidal shape. When the treatment duration was extended to 15 min, slight changes occurred in the fiber wall thickness and the morphology of the ellipsoidal starch particles. It was evident that the number of cracks in the cell walls had increased, and their lengths had become longer. At 270 ℃ and after 10 min, this cracking became more pronounced, with cracks nearly penetrating the entire cell wall. At this stage, the starch underwent considerable pyrolysis and turned into a paste-like substance that adhered to the inner wall of the lumina or the wood rays. Following at 270 ℃ and after 15 min, the cracking of the cell walls intensified further, with the true middle lamella separation, and

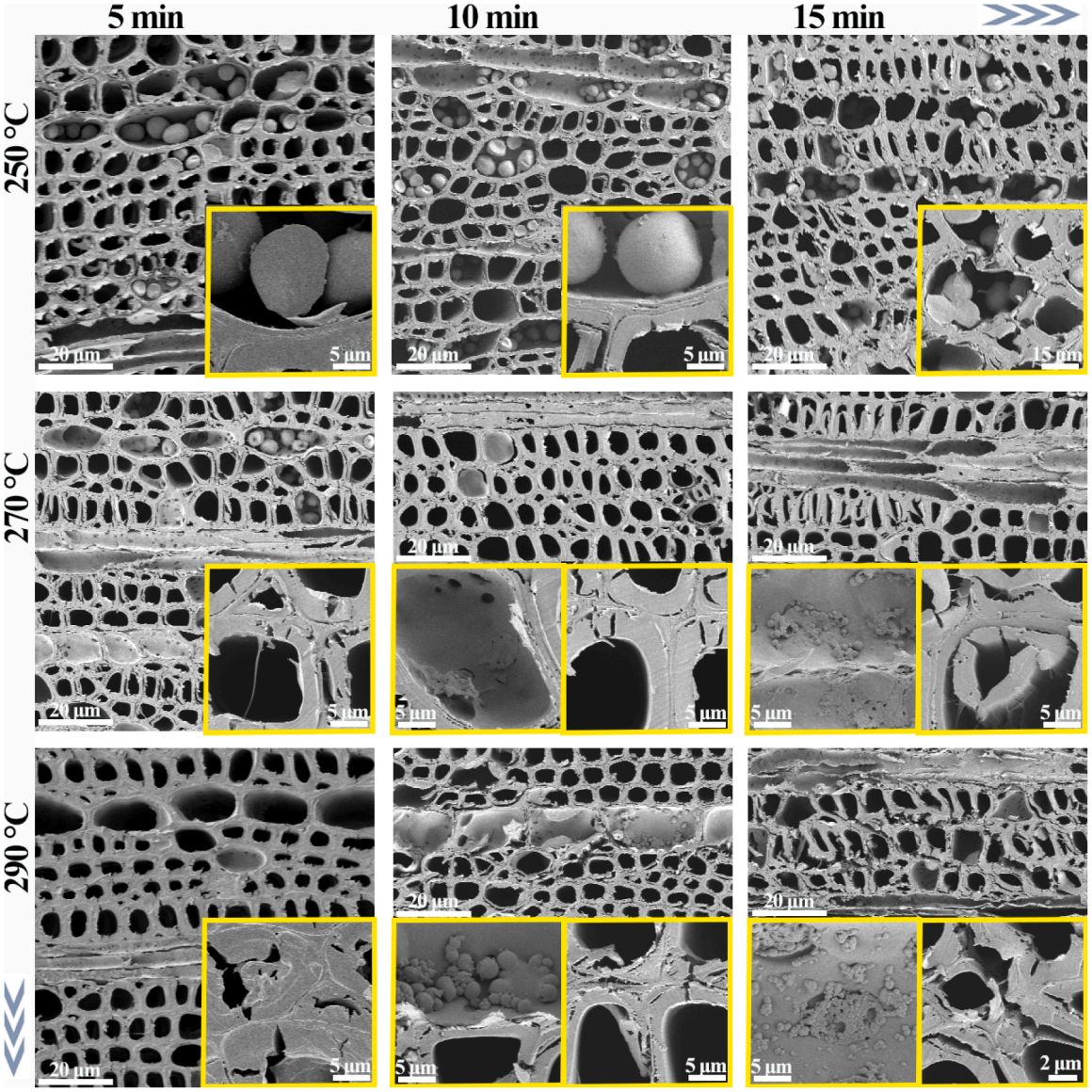

Fig. 2. SEM micrographs perpendicular to the fiber direction (L-direction) of rubberwood samples at different heat-treatment conditions.

the pyrolysis of starch continued to accelerate. After treatment at 290 ℃ for 10–15 min, the fibers became more brittle. Cracking and separation occurred in most of the treated areas, and the starch was almost completely pyrolyzed. As the cell walls rapidly lose water and the degradation of components leads to increased mass loss, these changes cause the cell walls to shrink and form cracks, thereby weakening the wood structure. All biopolymers in wood degrade at high temperatures, yet the rate of degradation varies, with hemicellulose degrading the most rapidly (Dömény et al., 2017; Huang et al., 2025).

3.3. Physical properties analysis

3.3.1. Dimensional stability analysis

The dimensional stability of the sample was assessed by measuring its dry shrinkage rate and swelling rate at different equilibrium moisture contents. As shown in Figs. 3a and 3b, the tangential, radial, and volumetric shrinkage rates of rubberwood, both towards air-dried and absolute-dried states, showed a decreasing trend upon increasing temperature and time. The maximum decrease in the air-drying process at 250 °C, 270 °C and 290 °C were 7 %, 21 % and 36 % in the tangential direction, 9 %, 7 % and 29 % in the radial direction, and 15 %, 17 % and 36 % in volume, respectively (Table SI-3), while the maximum decrease in absolute-drying process at 250 °C, 270 °C and 290 °C were 7 %, 6 % and 35 % in the tangential direction, 7 %, 11 % and 28 % in the radial direction, and 3 %, 6 % and 33 % in volume, respectively (Table SI-4). In a similar way, Figs. 3c and 3d show the tangential, radial, and volumetric thickness swelling rate of rubberwood, both towards air-dried and absolute-dried states, where a decrease in these parameters is observed upon increasing temperature and time. The maximum decrease from the air-drying process at 250 °C, 270 °C and 290 °C were 1 %, 4 % and 26 % in the tangential direction, 4 %, 10 % and 39 % in the radial direction, and 10 %, 12 % and 35 % in volume, respectively (Table SI-5), while the maximum decrease from the absolute-drying process at 250 °C, 270 °C and 290 °C were 41 %, 44 % and 57 % in the tangential direction, 26 %, 30 % and 51 % in the radial direction, and 40 %, 44 % and 58 % in volume, respectively (Table SI-6). In all cases, the four studied dimensional parameters show a maximum decrease at 290 °C and after 15 min of heat treatment.

After heat treatment, the hydrophilicity of rubberwood decreases, significantly enhancing its stability. This improvement in stability also reduces the risk of cracking and bending defects during subsequent use. This improvement was attributed to the fact that the contact surface in

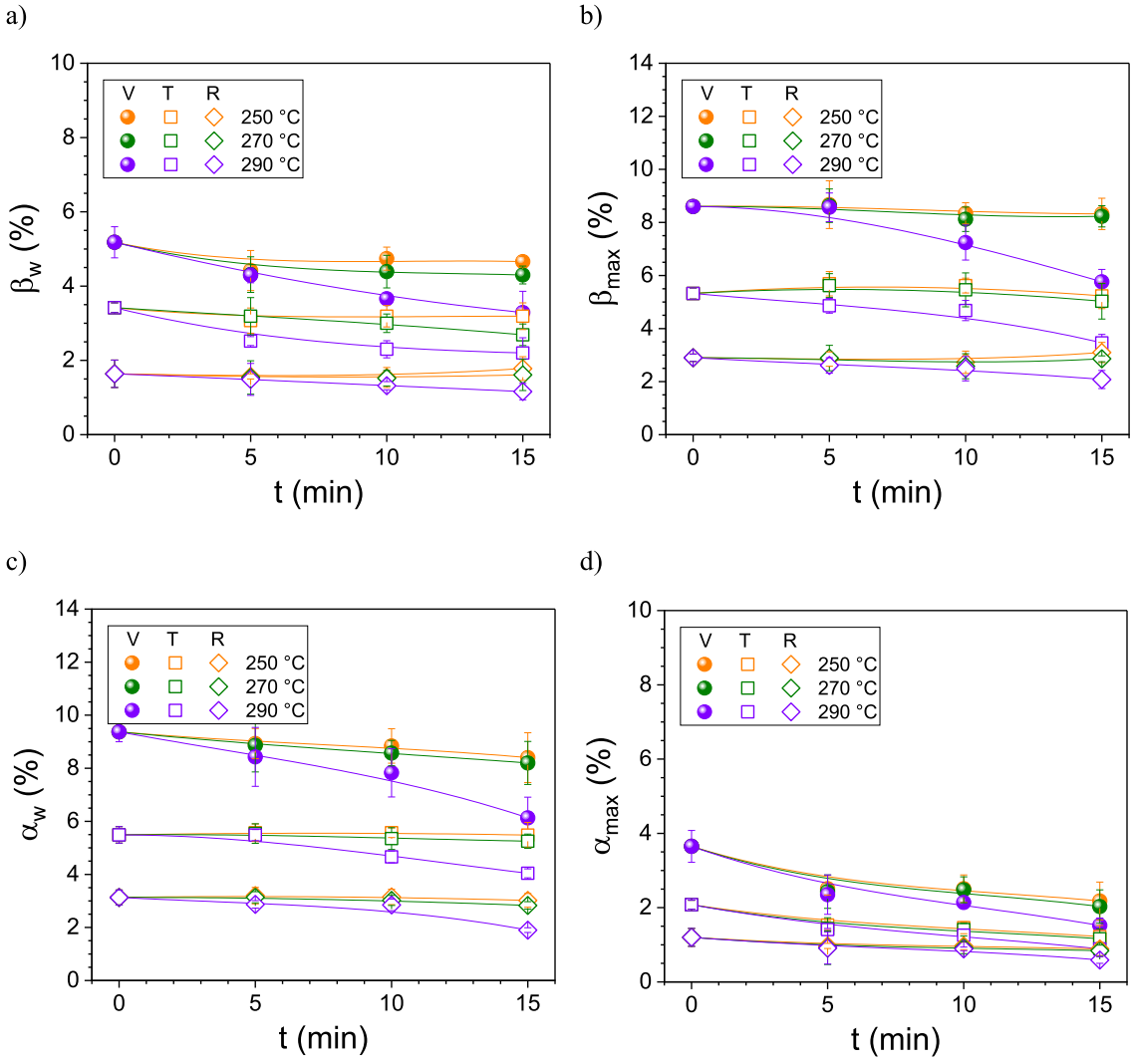

Fig. 3. Kinetics curves for the volumetric (V), tangential (T) and radial (R) drying shrinkage rate of the rubberwood samples treated at 250 °C, 270 °C and 290 °C from a) waterlogged wood to air-dried wood β_w, and b) air-dried wood to absolute-dried wood β_{max}. Kinetics curves for the volumetric (V), tangential (T) and radial (R) thickness swelling rate of the rubberwood samples treated at 250 °C, 270 °C and 290 °C from c) air-dried wood to waterlogged wood α_w, and d) absolute-dried wood to air-dried wood α_{max}.

the heated plate method was the tangential surface, where the thermal decomposition of the chemical components of wood was more pronounced compared to the radial surface. As a result, the dimensional stability changes in the radial and tangential directions differ, reducing the discrepancy in dry shrinkage and swelling between these two directions. In this study, only the surface of the wood was treated, yet its stability was still superior to that of wood treated with conventional overheated steam. Moreover, this treatment method offers greater advantages in terms of processing efficiency and energy consumption (Laine et al., 2012).

3.3.2. Density profiles analysis

To analyze the effect of the heated plate method on the internal density distribution of the sample, a density profile measurement was performed. The density profile curves of the samples are shown in Fig. 4, and the analysis of the density profile was conducted by adjusting the data to a double-exponential decay function (Fig. SI-4 and Table SI-7). From the data obtained, it is clearly evident that the surface of the sample has been compressed, as indicated by the increased density (Δρ) at both extremes of the samples and the reduced distance (d) due to compression of the heated surfaces of the wood. Sample thickness varied significantly with the processing parameters, showing a consistent decrease with elevated temperature and prolonged treatment duration (Fig. 4b), reaching up to 11 % of thickness reduction at 290 °C and after 15 min of heat treatment. The density increase on the surface was also analyzed and the results are shown in Fig. 4c. The average density increase value was also a function of temperature and processing time, showing a maximum increase of 524 Kg/m^3 above the average density value of rubberwood (ρ = 665 Kg/m^3) was achieved at 290 °C and after 15 min of heat processing. However, the density inside the sample remained nearly the same as the original density of the wood. This is because the treatment temperature and processing time were not enough to degrade the amorphous hemicelluloses and cellulose in the cell wall domains. Under mechanical force, the softened tube cavities on the wood surface were compressed and compacted. This softening and compression process likely occurred within a very short time frame. As the treatment duration increases, the three main components of the wood undergo pyrolysis, significantly enhancing the plasticity of the wood. The previous method of fixing the deformation of compressed wood required heat treatment of the entire wood (Laine et al., 2016). The method presented in this paper may offer a new solution for fixing compressed wood.

3.4. Mechanical analysis

3.4.1. MOE and MOR analysis

The modulus of elasticity (MOE) and the modulus of rupture (MOR) serve as the critical indicators for evaluating the mechanical properties if degradation is present upon heat treatment, directly influencing its potential application value. The trends in MOR and MOE are closely linked to the heat treatment conditions. As the treatment temperature and the treatment duration increased, both MOR and MOE of the wood generally decreased, as shown in Fig. 5a and b (Table SI-8). A comparative analysis revealed differential response patterns between these mechanical parameters. While both properties were temperature-dependent, MOR displayed greater sensitivity to heat treatment, showing a more significant decrease than MOE at all temperature levels. For long processing times, both MOE and MOR tend to reach a stabilization plateau. The relative MOE values at 250 °C, 270 °C and 290 °C after 15 min heat treatment decrease 2 %, 3 % and 11 %, respectively, while the relative MOR values, at the same treatment temperature and for 15 min, decrease 29 %, 31 % and 47 %, respectively.

The majority of wood samples prepared via the heated platen modification method reached the TB.11–20 strength grade requirements according to Chinese National Standard GB 50206–2012. Only those treated at 290 ℃ for 10–15 min failed to meet the minimum strength

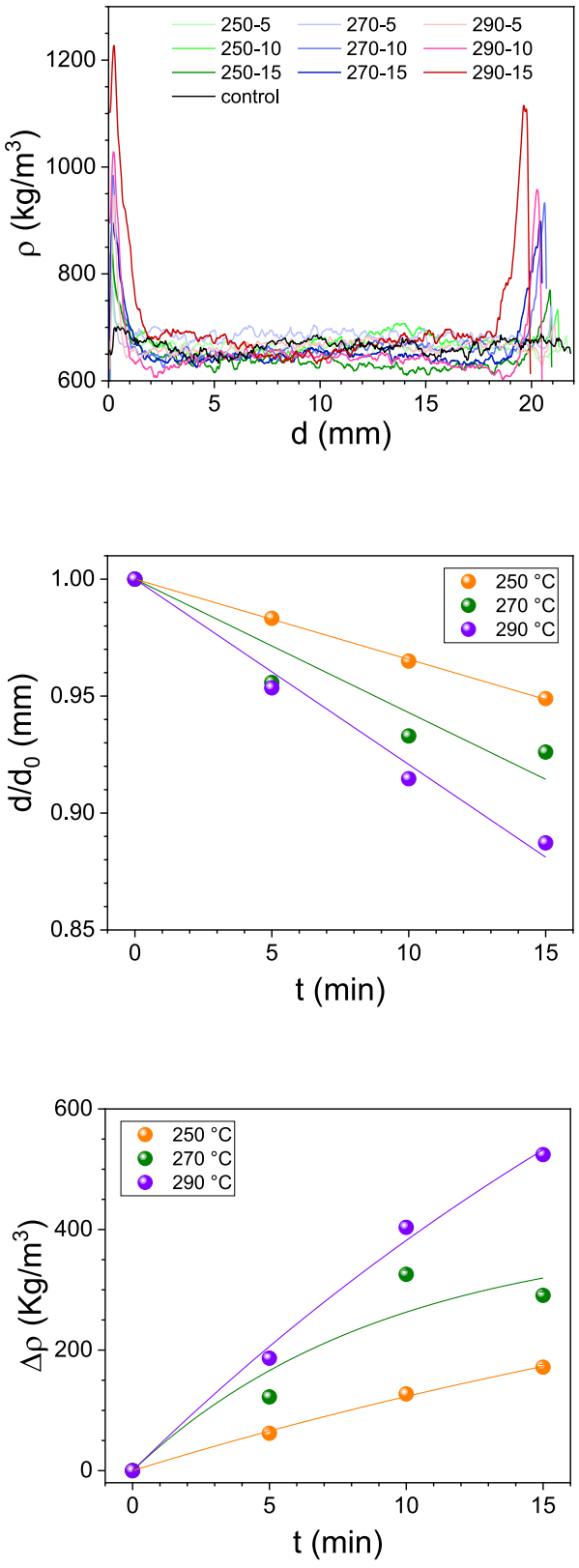

Fig. 4. a) Density profile for the rubberwood samples treated at 250 °C, 270 °C and 290 °C after 5, 10 and 15 min of heat treatment. b) Relative thickness decrease analysis and c) density increase at the extremes of the rubberwood samples.

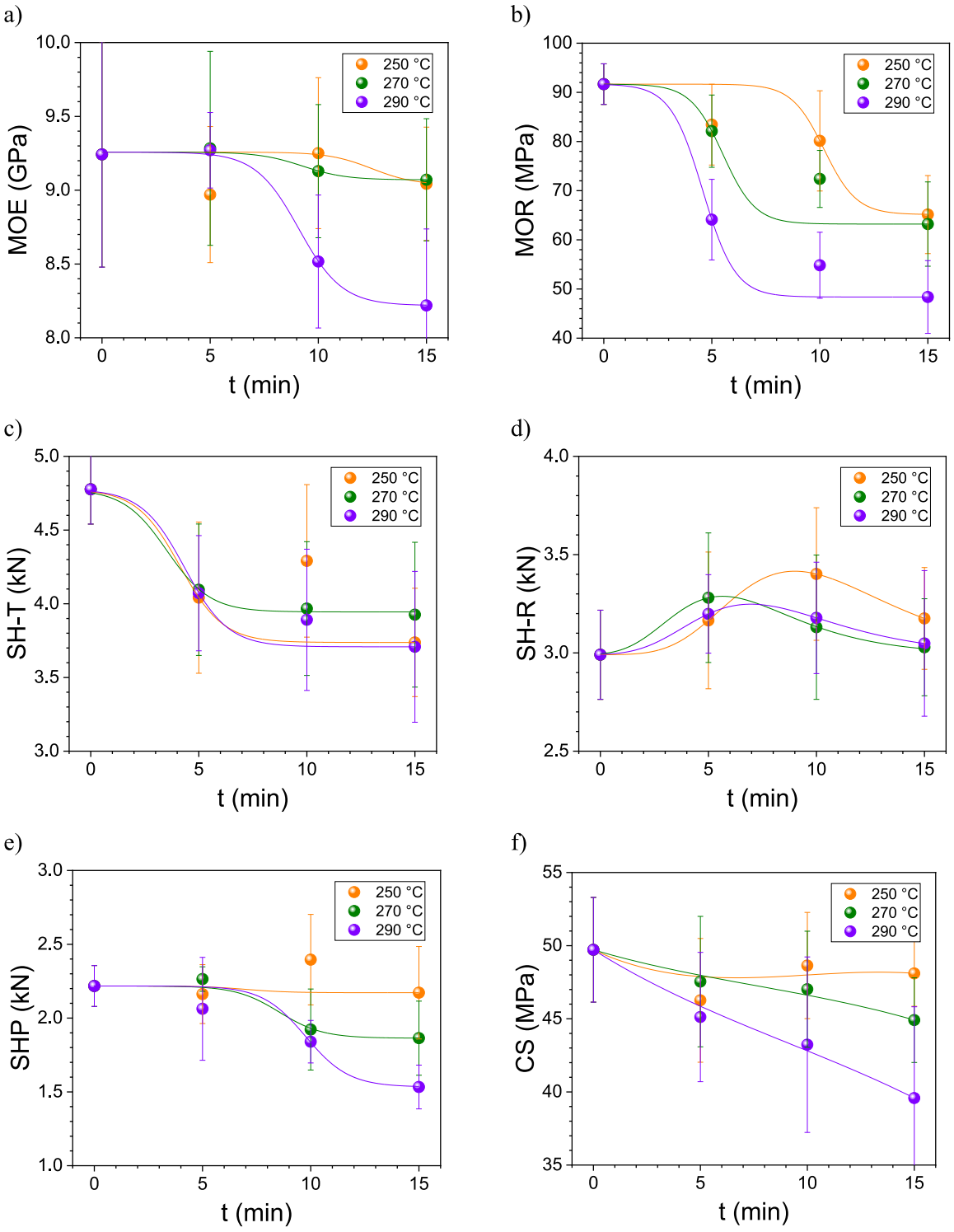

Fig. 5. a) Modulus of elasticity (MOE), b) modulus of rupture (MOR), c) surface hardness in the tangential direction (SH-T), d) surface hardness in the radial direction (SH-R), e) screw holding power (SHP), and d) compressive strength (CS) parallel to grain direction for the rubberwood samples treated at 250 °C, 270 °C and 290 °C after 5, 10 and 15 min of heat treatment.

criteria, while all other treatment conditions conformed to structural application standards. Consequently, heated platen-modified rubberwood was particularly well-suited for non-structural or semi-structural applications where dimensional stability was paramount, such as indoor furniture and interior floor requiring resistance to warping under varying humidity conditions under primarily static loads. In summary, this modified wood demonstrates significant potential as a value-added material for furniture manufacturing and building construction applications.

The increase in percentage of the cellulose crystallinity due to the loss of amorphous components can also offset the mechanical property degradation caused by the initial heat treatment. As treatment temperature and duration increase, thermal degradation initiates in hemicellulose, followed by progressive breakdown of lignin and crystalline

cellulose. Functioning as a natural interfacial coupling agent within the cell wall, hemicellulose provides both filler material and adhesive bonding between lignin and cellulose microfibrils. Its thermal decomposition critically compromises this interfacial adhesive function, affecting stress transfer under load. As a result, the static bending strength of the wood is significantly reduced. (Muzamal et al., 2017; Zauer et al., 2016). This reduction was macroscopically manifested as a decrease in both MOE and MOR. At the microstructure level, this phenomenon is evident through cell wall deformation and cracks in the true middle lamella.

3.4.2. Surface hardness analysis

Surface hardness plays an important role in heat-treated wood, particularly that used as solid wooden flooring or furniture. Heated platen treatment can reduce the surface hardness of the tangential section; however, within a certain temperature and duration range, it can increase the surface hardness of the radial section as shown in Figs. 5c and 5d (Table SI-8). Quantitative analysis of the surface hardness disclosed fundamentally different temporal evolution patterns for the two hardness orientations. SH-T asymptotically approached equilibrium hardness values with prolonged exposure, whereas SH-R manifested a characteristic peak at approximately 10 min before commencing decay. This phenomenon can be explained by the structural transformation of lignin during treatment. In the early stages of treatment, the extensive degradation of polysaccharides increased the relative content of lignin and crystalline cellulose. As the treatment temperature and duration increased, while lignin did not undergo significant degradation, its molecular structure underwent reorganization. This structural rearrangement resulted in the formation of a more stable cross-linked network that encapsulated microfibril surfaces, enhancing their ability to withstand compressive loads along the grain (Brosse et al., 2010; Sun et al., 2022). Wang *et al.,* through infrared imaging and nano-indentation, revealed a strong correlation between lignin redistribution patterns and cell wall hardness evolution (Wang et al., 2022).

3.4.3. Screw holding power analysis

Screw holding power (SHP) refers to the resistance of wood materials to pull out a screw. It is a crucial property in the design of wooden structures with screw connections, as it helps secure the screw and prevent it from being pulled out by external forces. As shown in Fig. 5e, when the treatment temperature was 250 ℃, the screw holding power exhibited a trend of initially increasing and then decreasing with the extension of the treatment duration. After 15 min of processing, the effect of the treatment temperature became more pronounced. The relative SHP values at 250 °C, 270 °C and 290 °C after 15 min heat treatment decrease 2 %, 16 % and 31 % (Table SI-8), respectively, suggesting a big change in the polymers' composition at high temperature and reaching a plateau value for longer processing times. The changes in lignin and hemicellulose significantly affect SHP. Lignin serves as the primary filler and hardening substance in the cell wall, while hemicellulose functions as an interfacial coupling agent that connects lignin and cellulose, playing a role in filling and partially binding components within the cell wall (Berglund et al., 2020). Changes in the contents of these two substances may affect the mechanical interlocking strength between the screw and the wood, as well as the friction between them. The compositional analysis results demonstrated a correspondence with the observed fluctuations in SHP. However, current research has primarily focused on the influence of macroscopic properties of wood, such as wood species, density, moisture content, and controllable screw factors, on screw holding power. There has been less exploration of the mechanisms at the nanoscale, which will require further research.

3.4.4. Compressive strength analysis

As a structural material for furniture manufacturing, wood's load-bearing capacity predominantly depends on its compressive strength (CS) parallel to the grain direction. Accordingly, the CS of the rubberwood samples under different heat-treatment conditions and the control sample were measured (Table SI-8). As shown in Fig. 5f, the relative CS values at 250 °C, 270 °C and 290 °C after 15 min heat treatment decrease by 3 %, 10 % and 20 %, respectively, which are consistent with the observed changes in hardness. However, distinct variation patterns were observed between these two parameters. CS demonstrated pronounced sensitivity to both thermal processing parameters (temperature and duration), as clearly illustrated in the performance kinetics curve. ANOVA results demonstrated that both treatment temperature and duration significantly affected MOR and CS. Notably, the effect on MOR was highly significant ($P < 0.01$), with treatment temperature having a more pronounced influence on both MOR and CS than treatment duration.

3.5. Wood color analysis

The chromatic evolution of heat-treated wood represents a critical quality indicator. The aesthetically pleasing texture developed during treatment significantly enhances consumer appeal, while these color variations directly correlate with underlying changes in chemical composition, physical and mechanical properties. Fig. 6a compares the surface color between heat-treated samples and the control sample. Rubberwood darkened progressively with increasing temperature/duration, approaching indistinguishable dark brown at 290 ℃ for 10 min and longer processing times. The surface color of the high-temperature, short-term treatment process was similar to that of the low-temperature, long-term treatment process.

Fig. 7 indicates the changes in the color characteristic as a function of the processing temperature and time (Table SI-9). L^* values decreased as temperature and duration increased, with a relative decrease at 250 °C, 270 °C and 290 °C after 15 min of heat treatment of 37 %, 44 % and 49 %, respectively. The a^* value mirrored visual changes with an increase of 24 %, 35 % and 61 % after 15 min at 250 °C, 270°C and 290 °C, respectively, whereas it was opposite to b^* with a decrease of 20 %, 32 % and 44 %, respectively. The ΔE^*, which most effectively reflected the changes in surface color after treatment, showed a pattern similar to that of L^* value but with a positive correlation, as shown by the kinetics curve. A notable observation was that, at the same processing temperature, the color difference increased sharply with longer durations. ANOVA revealed that both temperature and duration significantly affected L^* and ΔE^*, with duration having a greater impact, yet neither parameter significantly affected a^*.

During the treatment, the changes in the surface color of rubberwood are closely related to alterations in the structure and content of lignin. Lignin undergoes discoloration reactions under high-temperature conditions. Specifically, acid-insoluble lignin begins to undergo a thermal color change at temperatures as low as 140 ℃, with the color gradually turning brown as the temperature increases. In heated platen treatment, acetic acid generated from the degradation of hemicellulose acts as a catalyst, promoting the continuous increase in phenolic hydroxyl groups formed by acid-soluble lignin during heat treatment (Sundqvist et al., 2006; Zhu et al., 2024c). This results in enhanced absorbance and further color changes. Simultaneously, the extractives in the rubberwood continue to decompose, producing new chromophores that deepen the color, reduce the value of L^*, and increase the value of ΔE^*.

3.6. Surface natural decay resistance analysis

Wood decay is primarily caused by fungal infection, where microbial proliferation degrades the structural components of wood, resulting in the loss of rigidity. Table 1 presents the average mass loss rate for the treatment group and the control group after twelve weeks of exposure to the white-rot fungi and brown-rot fungi; the mass loss rates of the treatment group were significantly lower than those of the untreated control, which were 11.6 % and 7.1 %, respectively. Notably, white-rot

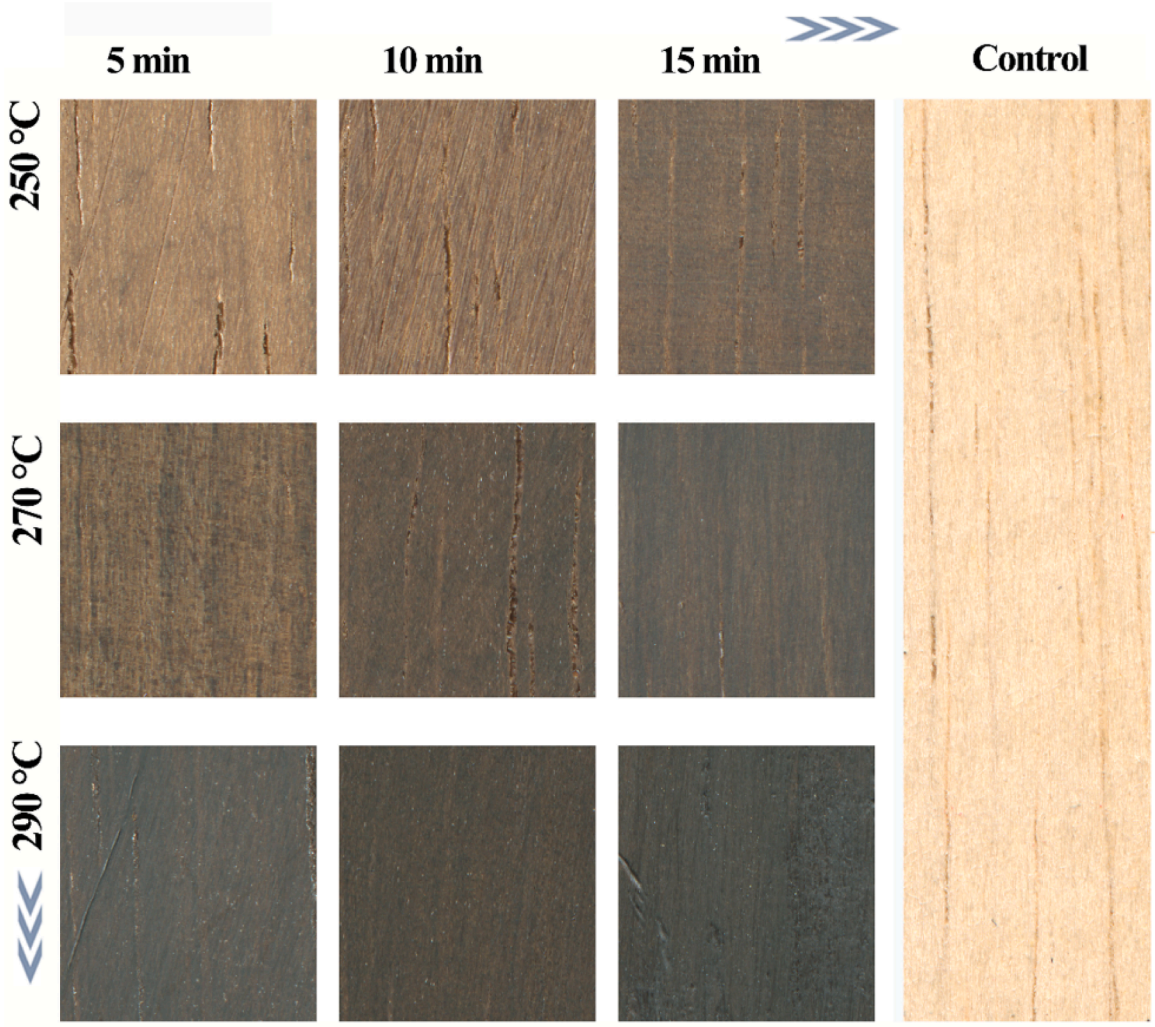

Fig. 6. The surface color of rubberwood samples treated at 250 °C, 270 °C and 290 °C after 5, 10 and 15 min of heat treatment.

fungi caused significantly greater mass loss than the brown-rot fungi across all treatment groups. This pattern was consistent with previous studies, as white-rot fungi comprehensively degrade all wood components, with a preferential breakdown of lignin, whereas brown-rot fungi primarily target cellulose and hemicelluloses while causing limited lignin degradation (Goodell et al., 2017). Consequently, although brown-rot fungi result in lower mass loss, they cause more severe structural damage due to cellulose depletion.

From the values in Table 1, and assuming an exponential decay $m(t)/m_0 = e^{-t/\tau}$, the lifetime for each rubberwood sample could be calculated, allowing for the simulation of the decay behavior for each heat treatment. Fig. 8a and b depict the corresponding decay curves for all rubberwood samples and the corresponding control sample when exposed to white-rot fungi and brown-rot fungi, respectively. Even though there is no clear trend between the heat-treated samples, all of them fall above the corresponding control sample, indicating that heat treatment reduces the decay behaviour due to changes in the chemical composition and molecular structure of the wood components.

In order to better understand the decay behaviour between the different heat treatment conditions, the lifetime values were plotted as a function of time, as shown in Figs. 8a and 8b. For both fungi tests, a maximum in the lifetime value can be localized, which can be attributed to the optimal processing time for each temperature. For the white-rot fungi test, the optimal processing time at 250 °C, 270 °C and 290 °C is 13.1, 8.7 and 7.1 min, respectively, whereas for the brown-rot fungi test, the optimal processing time is 1.5, 9.3 and 8.1 min, respectively. Therefore, any time applied below or above these optimal values results in lower decay time and, thus, lower resistance to the fungi exposure. This seems to be the case where, above the optimal processing times, the wood components suffer some chemical transformation to make the wood more resistant than the control sample, but still edible for the fungi. At processing times above the optimal value, wood degrades more and makes it easier the access to the fungi to components hidden in the core of the cell wall.

Microstructural analysis revealed that elevated temperatures and extended durations led to microfractures in the cell walls, ultimately causing fiber embrittlement. These microcracks facilitate fungal hyphae penetration and colonization. Since the interior of the rubberwood remains largely unmodified, it becomes highly susceptible to decay (Dubey et al., 2016). Thus, specimens subjected to high-temperature/long-duration treatments exhibited reduced decay resistance. This enhanced resistance can be attributed to several mechanisms resulting from thermal modification. Firstly, the heat treatment process forms a protective surface layer while simultaneously degrading a substantial portion of hemicellulose and modifying the edible monomers in wood biopolymers, thereby reducing the availability of easily degradable substrates for fungal colonization and growth (Jiang et al., 2022). Secondly, the cross-linking and reorganization of lignin polymers lower the concentration of water-absorbing functional groups in the wood matrix, creating less favorable conditions for fungal development (Mohareb et al., 2011; Zhao, X. et al., 2024b). Additionally, under the closed, pressurized conditions of thermal modification, various reaction

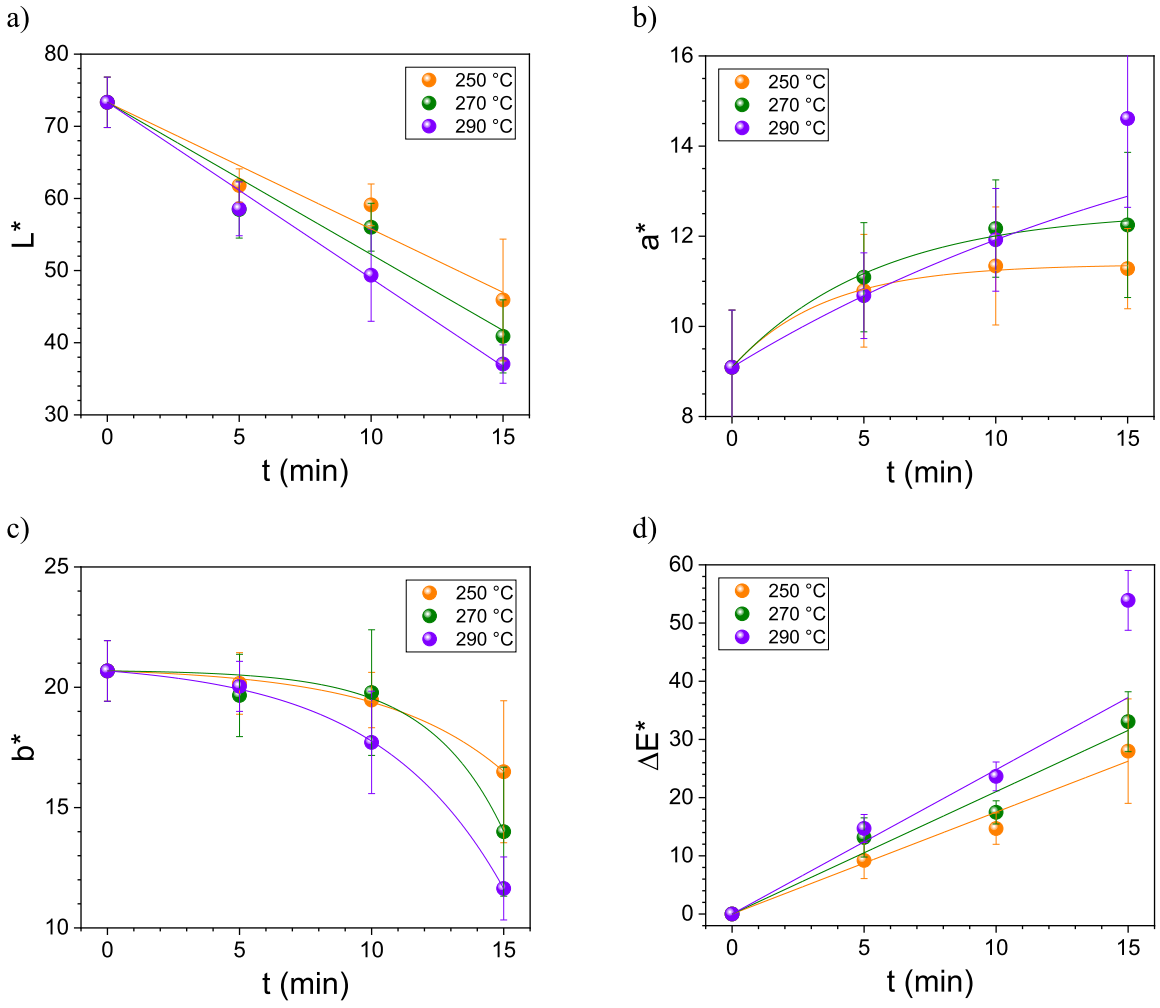

Fig. 7. The color characteristics (L*, a*, b* and ΔE*) of rubberwood samples treated at 250 °C, 270 °C and 290 °C after 5, 10 and 15 min of heat treatment.

Table 1
The mass loss rate of the treatment group and the control group after 12 weeks of natural decay resistance test of rubberwood samples treated at 250 °C, 270 °C and 290 °C after 5, 10 and 15 min of heat treatment.

sample	t (min)	White-rot fungi		Brown-rot fungi	
control		11.6	± 0.6	7.1	± 0.6
250 °C	5	8.7	± 0.9	4.9	± 0.9
	10	7.5	± 0.6	4.7	± 0.8
	15	7.1	± 0.9	4.6	± 0.4
270 °C	5	8.1	± 0.8	4.8	± 0.7
	10	7.1	± 0.5	4.5	± 0.9
	15	8.6	± 0.4	4.8	± 0.2
290 °C	5	7.6	± 0.4	4.5	± 0.5
	10	8.3	± 0.8	4.7	± 0.4
	15	9.1	± 1.1	5.0	± 0.5

Notes: a mean value ± standard deviation.

products remain trapped within the wood structure. These include furan derivatives and phenolic compounds with known antifungal properties, which persist in the modified wood and contribute to fungal growth inhibition (Candelier et al., 2016).

3.7. Correlation analysis

As mentioned previously, the properties of thermally modified rubberwood through the heated platen method were significantly influenced by both treatment temperature and duration. To rapidly evaluate performance variations and identify the most strongly correlated indicators, Pearson correlation analysis was conducted. Fig. 9a presents the results of the correlation analysis, encompassing mechanical properties, compositional characteristics, dimensional stability, surface color changes, and decay resistance across all treatment conditions.

The analysis revealed several strong correlations between color parameters and material properties. The total color difference (ΔE^*) showed significant negative correlations with mechanical properties, including MOR (r = -0.927), SH-T (r = -0.892), and SHP (r = -0.835), indicating that greater color darkening corresponds to more pronounced mechanical deterioration. Conversely, b^* demonstrated positive correlations with these mechanical properties (MOR: r = 0.842; SH-T: r = 0.789; SHP: r = 0.762), suggesting that cellulose integrity contributes to both mechanical performance and yellower coloration. Particularly, strong correlations were observed between color parameters and chemical composition, with LC showing high correlation with both ΔE^* (r = 0.941) and b^* (r = -0.883), while HC correlated strongly with ΔE^* (r = -0.921). Dimensional stability parameters also exhibited notable correlations, with α_{maxV} showing strong negative correlations with both ΔE^* (r = -0.879) and b^* (r = -0.812).

Based on the concept of non-destructive testing, we propose utilizing surface color parameters of rubberwood as indirect indicators of performance changes after heat treatment. Pearson correlation analysis revealed significant positive correlations between L^* and b^* with most

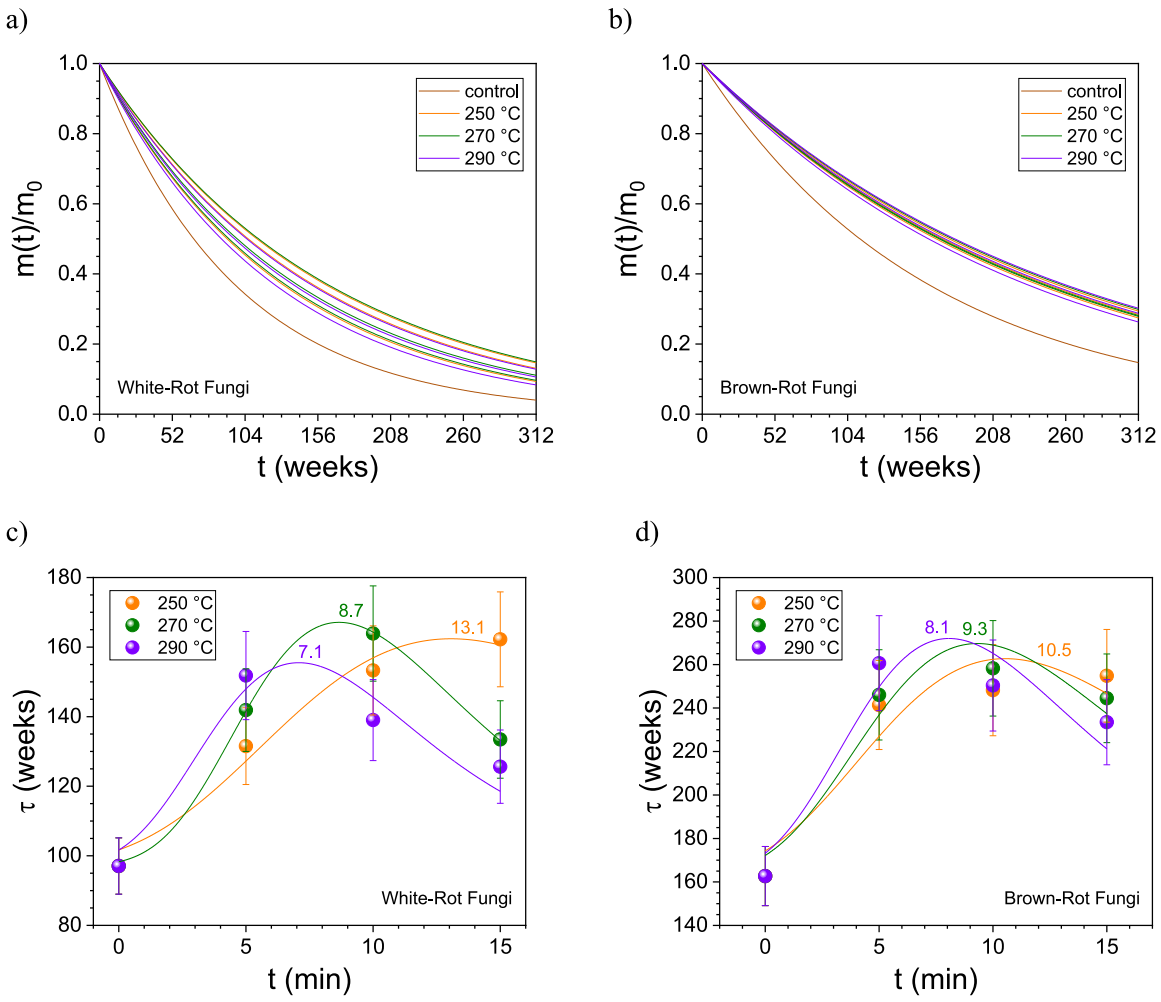

Fig. 8. Decay curves for the rubberwood samples treated at 250 °C, 270 °C and 290 °C after 5, 10 and 15 min of heat treatment and the corresponding control sample calculated from the data obtained in the a) white-rot fungi and b) brown-rot fungi tests. Lifetime values as a function of processing time at 250 °C, 270 °C and 290 °C after 5, 10 and 15 min of heat treatment from the data obtained in the a) white-rot fungi and b) brown-rot fungi tests.

mechanical properties. Notably, the ΔE^* demonstrated significant negative correlations with all mechanical properties ($|r|$=0.648–0.927), suggesting that greater color changes correspond to more pronounced mechanical deterioration. The positive correlations between b^* and mechanical properties ($r = 0.672$–0.842) may originate from the association between increased yellowness (due to lignin degradation during heat treatment) and mechanical performance. Cellulose content exhibited highly significant positive correlations with b^* ($r = 0.854$, $p = 0.003 < 0.01$), confirming cellulose's contribution to lighter, yellower wood coloration. Furthermore, swelling and shrinkage coefficients showed strong negative correlations with ΔE^*, demonstrating that color change can predict dimensional stability. However, the correlation between the mass loss and various performance indicators was relatively weak. Therefore, the comprehensive assessment system for the loss rate still requires further investigation.

The average correlation coefficients using b^* and ΔE^* as reference sequences are shown in Figs. 9b and 9c, respectively. The remarkably similar rankings obtained from both reference sequences, as evidenced by nearly identical radar chart patterns, confirm the robustness of these color parameters as indicators. Among the 11 evaluated parameters, only MOE showed relatively weak correlations. Subsequently, multiple linear regression analysis was performed to establish predictive models for key performance metrics using ΔE^* and b^* as independent variables. The regression equations and the corresponding correlation coefficients (R^2) are summarized in Table 2. All developed models exhibited high R^2 values, ranging from 0.698 to 0.902, indicating that the color parameters effectively explain a substantial portion of the variance in the measured properties.

The regression analysis, as shown in Table 2, demonstrated that in all established models, ΔE^* had P-values below 0.001 and generally exhibited higher standardized coefficients compared to b^*. This finding underscored that color darkening induced by heat treatment was the most sensitive indicator for predicting wood property alterations, including reductions in mechanical strength and chemical composition changes. The highest R^2 value (0.902) was observed for lignin content, strongly supporting that the color development was predominantly driven by chemical transformations, *e.g.*, condensation, redistribution, and relative enrichment of lignin. The negative correlation between ΔE^* and polysaccharide contents, *i.e.*, cellulose and hemicellulose, aligns with their degradation during treatment. These results provided a theoretical foundation for the non-destructive quality assessment of thermally modified wood using colorimetry.

Finally, in Table SI-10, the changes in crystallinity (χ), maximum volumetric drying shrinkage rate (β_{maxV}), maximum volumetric thickness swelling rate ($\alpha_{w\ maxV}$), modulus of elasticity (MOE), modulus of rupture (MOR), surface hardness (SH-T and SH-R), screw holding power (SHP), compressive strength (CS), mass loss rate of white-rot fungi (MLW), and mass loss rate of brown-rot fungi (MLB) of the rubberwood samples at different temperatures and heating times compared with the control sample are summarized for comparison.

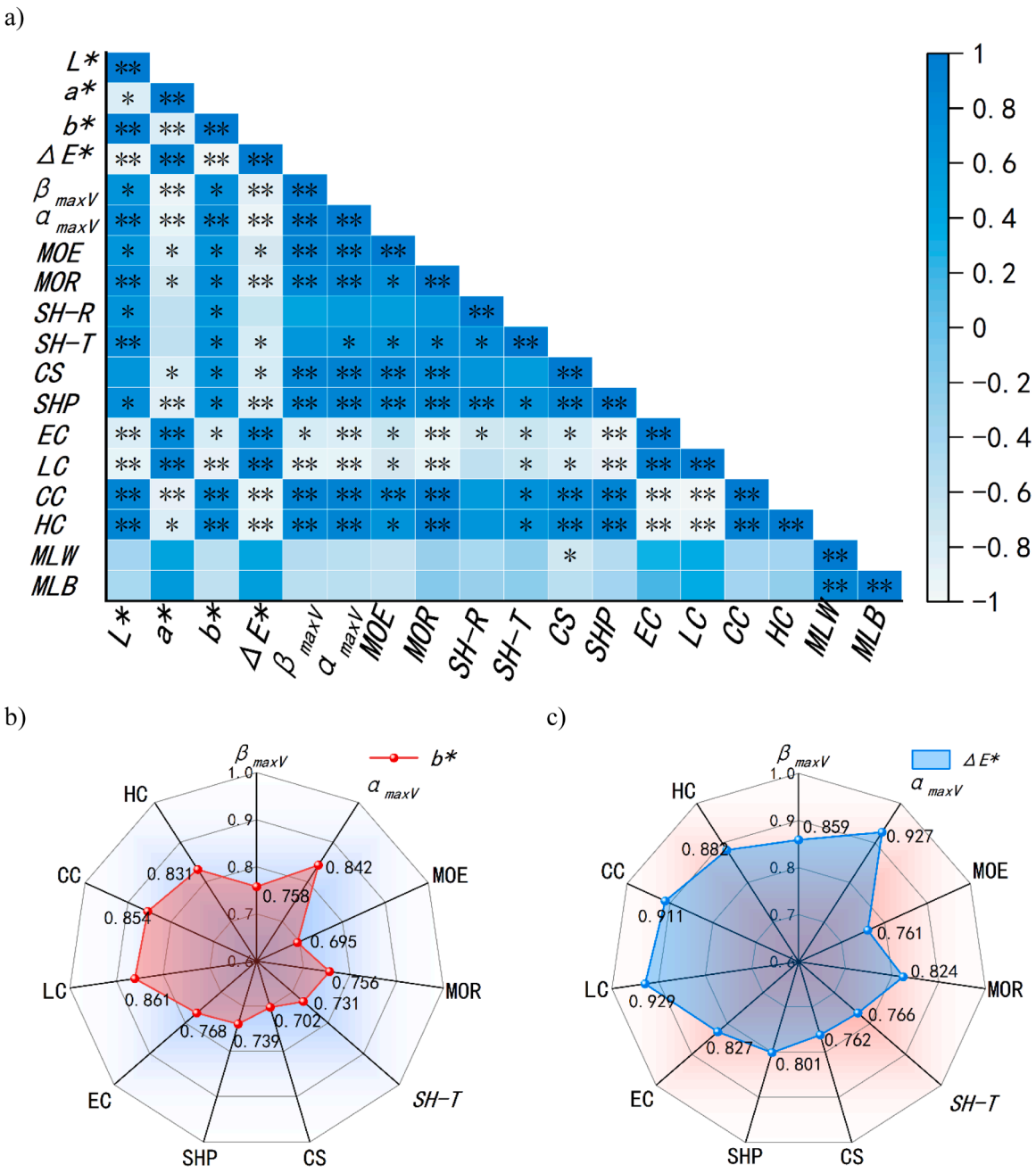

Fig. 9. a) Results of the correlation analysis. The correlation coefficients using b) b^*, and c) ΔE^* as reference sequences.

Table 2
The regression equations and the corresponding correlation coefficients (R^2) of the predictive models for key performance metrics using ΔE^* and b^* as independent variables.

Property	Regression Equation	R^2
Volumetric Shrinkage (β_{maxV})	$\beta_{maxV} = 3.87–0.28b^* + 0.35\Delta E^*$	0.812
Volumetric Swelling (α_{maxV})	$\alpha_{maxV} = 5.23–0.34b^* + 0.41\Delta E^*$	0.864
Modulus of Rupture (MOR)	$MOR = 32.14 + 1.25b^* - 0.87\Delta E^*$	0.782
Tangential Surface Hardness (SH-T)	$SH\text{-}T = 45.67 + 0.98b^* - 1.12\Delta E^*$	0.735
Screw Holding Power (SHP)	$SHP = 28.56 + 0.85b^* - 0.73\Delta E^*$	0.698
Lignin Content (LC)	$LC = 12.45–0.75b^* + 0.88\Delta E^*$	0.902
Cellulose Content (CC)	$CC = 68.33 + 0.92b^* - 0.65\Delta E^*$	0.831
Hemicellulose Content (HC)	$HC = 24.37 + 0.62b^* - 0.78\Delta E^*$	0.849

4. Conclusions

In summary, this paper investigated a rapid thermal modification method for rubberwood, which can be fully performed using a hot press. Compared to conventional thermally modified wood, this approach allows the production of materials with minimal mechanical loss, enhanced dimensional stability, and improved decay resistance, while maintaining the integrity of the bulk material. The study systematically evaluated heated platen-treated rubberwood through a comprehensive analysis of its chemical structure, chemical composition, microstructure, physical performance, mechanical performance, surface color, and natural decay resistance. Additionally, color parameters were used for non-destructive quality assessment of these properties. The main conclusions are as follows:

(1) The FTIR analysis revealed that hemicellulose degradation was the most prominent chemical change. WAXS analysis showed that as the

treatment temperature and duration increased, hemicellulose degradation reduced the amorphous content, raising the cellulose crystallinity from 40 % to 64 %. Components analysis corroborated these findings, with hemicellulose content decreasing by 25 %, 38 %, and 53 % at 250 ℃, 270 ℃, and 290 ℃ after 15 min, respectively. The increase in degradation products and their reduced proportion in the remaining material led to a higher content of extractives and lignin.

(2) Heated platen treatment resulted in significant improvements in both efficiency and performance retention. At the three treatment temperatures and after 15 min, MOR reduction was limited to 29–47 %, with only a 2–11 % loss in MOE and a 3–20 % reduction in CS. SH-R increased by 15–30 %, while SHP resistance decreased by only 2–31 %. The treated rubberwood showed remarkable dimensional stability improvements, with tangential shrinkage reduced by 7–36 % and volumetric swelling decreased by 40–58 % compared to the controls. Density profiles analysis revealed a maximum density increase on the surface of 524 kg/m^3 above the average rubberwood density.

(3) Rubberwood modified by heated platen treatment exhibited significantly enhanced fungal resistance, reducing mass loss from white-rot fungi from 11.6 % to 7.1 % and brown-rot fungi decay from 7.1 % to 4.5 %, representing *ca.* 35–40 % of decay reduction. Optimal decay protection was achieved at 270 ℃ for 10 min. By simulating the decay behavior of heat-treated wood, the optimal treatment durations for protection were further refined to 8.7 min and 9.3 min at 270 °C. However, prolonged high-temperature treatment induced micro-cracks in the cell walls, creating pathways for fungal invasion and resulting in increased mass loss.

(4) The thermal treatment caused a progressive darkening, with ΔE^* increasing proportionally to both temperature and duration. L^* values decreased by 37–49 %, while a^* increased by 24–61 %, and b^* decreased by 20–44 %. This study used color parameters for non-destructive quality assessment, revealing strong correlations between color differences and mechanical properties ($|r| = 0.648–0.927$), chemical composition (R^2 up to 0.902), and dimensional stability (R^2 up to 0.864). However, due to the complexity of decay resistance mechanisms, the chromatic parameters could not fully account for variations in fungal durability.

CRediT authorship contribution statement

Dengyun Tu: Writing – review & editing, Supervision, Resources, Funding acquisition, Conceptualization. **Antoni Sánchez-Ferrer:** Writing – review & editing, Writing – original draft, Visualization, Validation, Software, Methodology, Formal analysis, Data curation. **Wanli Cheng:** Writing – review & editing, Supervision, Resources, Funding acquisition. **Xiangyu Zhao:** Writing – review & editing, Investigation. **Qiaofang Zhou:** Writing – review & editing, Investigation. **Xiaoxue Song:** Writing – review & editing, Investigation. **Jingyao Zhao:** Writing – review & editing, Investigation. **Zhipeng Zhu:** Writing – review & editing, Writing – original draft, Visualization, Software, Methodology, Investigation, Formal analysis, Data curation, Conceptualization.

Declaration of Competing Interest

The authors declare that they have no known competing financial interests or personal relationships that could have appeared to influence the work reported in this paper

Acknowledgements

This work was supported by the Guangdong Forestry Science and Innovation Project (No. 2025KJCX011) and the National Natural Science Foundation of China (No. 32401501 and 32271786). Scientific Compass (www.shiyanjia.com) assisted with the XRD testing part of this work.

Appendix A. Supporting information

Supplementary data associated with this article can be found in the online version at doi:10.1016/j.indcrop.2026.122638.

Data availability

Data will be made available on request.

References

Ahmed, M.J., Wu, B., Sánchez-Ferrer, A., 2025. Anion exchangers prepared from graft polymerisation of microfibrillated cellulose using the reactive ionic liquid. J. Bioresour. Bioprod. https://doi.org/10.1016/j.jobab.2025.04.001.

Altgen, M., Willems, W., Militz, H., 2016. Wood degradation affected by process conditions during thermal modification of European beech in a high-pressure reactor system. Eur. J. Wood Wood Prod. 74, 653–662. https://doi.org/10.1007/s00107-016-1045-y.

Altgen, M., Willems, W., Hosseinpourpia, R., Rautkari, L., 2018. Hydroxyl accessibility and dimensional changes of *Scots pine* sapwood affected by alterations in the cell wall ultrastructure during heat-treatment. Polym. Degrad. Stab. 152, 244–252. https://doi.org/10.1016/j.polymdegradstab.2018.05.005.

Berglund, J., Mikkelsen, D., Flanagan, B.M., Dhital, S., Gaunitz, S., Henriksson, G., Lindström, M.E., Yakubov, G.E., Gidley, M.J., Vilaplana, F., 2020. Wood hemicelluloses exert distinct biomechanical contributions to cellulose fibrillar networks. Nat. Commun. 11. https://doi.org/10.1038/s41467-020-18390-z.

Borrega, M., Kärenlampi, P.P., 2007. Mechanical behavior of heat-treated spruce (Picea abies) wood at constant moisture content and ambient humidity. Holz als Roh und Werkst. 66, 63–69. https://doi.org/10.1007/s00107-007-0207-3.

Brosse, N., Hage, R.E., Chaouch, R., Petrissans, R., Dumarcay, R., Gerardin, R., 2010. Investigation of the chemical modifications of beech wood lignin during heat treatment. Polym. Degrad. Stab. 95, 1721–1726. https://doi.org/10.1016/j.polymdegradstab.2010.05.018.

Candelier, K., Dumarçay, S., Pétrissans, A., Pétrissans, M., Kamdem, P., Gérardin, P., 2013. Thermodesorption coupled to GC–MS to characterize volatiles formation kinetic during wood thermodegradation. J. Anal. Appl. Pyrolysis 101, 96–102. https://doi.org/10.1016/j.jaap.2013.02.006.

Candelier, K., Thevenon, M.-F., Petrissans, A., Dumarcay, S., Gerardin, P., Petrissans, M., 2016. Control of wood thermal treatment and its effects on decay resistance: a review. Ann. For. Sci. 73, 571–583. https://doi.org/10.1007/s13595-016-0541-x.

Chen, S., Obataya, E., Matsuo-Ueda, M., 2018. Shape fixation of compressed wood by steaming: a mechanism of shape fixation by rearrangement of crystalline cellulose. Wood Sci.Technol. 52, 1229–1241. https://doi.org/10.1007/s00226-018-1026-x.

Ditommaso, G., Gaff, M., Kačík, F., Sikora, A., Sethy, A., Corleto, R., Razaei, F., Kaplan, L., Kubš, J., Das, S., Kamboj, G., Gašparík, M., Šedivka, P., Hýsek, Š., Macků, J., Sedlecký, M., 2020. Interaction of technical and technological factors on qualitative and energy/ecological/economic indicators in the production and processing of thermally modified merbau wood. J. Clean. Prod. 252. https://doi.org/10.1016/j.jclepro.2019.119793.

Dömény, J., Čermák, P., Koiš, V., Tippner, J., Rousek, R., 2017. Density profile and microstructural analysis of densified beech wood (*Fagus sylvatica* L.) plasticized by microwave treatment. Eur. J. Wood Wood Prod. 76, 105–111. https://doi.org/10.1007/s00107-017-1173-z.

Dubey, M.K., Pang, S., Chauhan, S., Walker, J., 2016. Dimensional stability, fungal resistance and mechanical properties of radiata pine after combined thermo-mechanical compression and oil heat-treatment. Holzforschung 70, 793–800. https://doi.org/10.1515/hf-2015-0174.

Engelhardt, M., Gilg, H.A., Richter, K., Sanchez-Ferrer, A., 2024. Adhesion-related properties of silver birch (Betula pendula Roth) wood as affected by hydrophilic extraction. Wood Sci. Technol. 58, 379–402. https://doi.org/10.1007/s00226-023-01526-x.

Esteves, B., Marques, A.V., Domingos, I., Pereira, H., 2006. Influence of steam heating on the properties of pine (Pinus pinaster) and eucalypt (Eucalyptus globulus) wood. Wood Sci. Technol. 41. https://doi.org/10.1007/s00226-006-0099-0.

Friend, A.D., Eckes-Shephard, A.H., Tupker, Q., 2022. Wood structure explained by complex spatial source-sink interactions. Nat. Commun. 13. https://doi.org/10.1038/s41467-022-35451-7.

Goodell, B., Zhu, Y., Kim, S., Kafle, K., Eastwood, D., Daniel, G., Jellison, J., Yoshida, M., Groom, L., Pingali, S.V., O'Neill, H., 2017. Modification of the nanostructure of lignocellulose cell walls via a non-enzymatic lignocellulose deconstruction system in brown rot wood-decay fungi. Biotechnol. Biofuels 10. https://doi.org/10.1186/s13068-017-0865-2.

Haseli, M., Efhamisisi, D., Abdulkhani, A., Oladi, R., Ungerer, B., Al-musawi, H., Halmschlager, E., Müller, U., 2024. Effects of oil heat treatment on poplar wood properties: a pilot scale study. Constr. Build. Mater. 430. https://doi.org/10.1016/j.conbuildmat.2024.136353.

He, L., Zhang, T., Zhao, Y., Gao, J., Zhang, Y., Yang, Y., He, Z., Yi, S., 2022. Effect of natural tung oil on wood shrinkage during the thermal modification process. J. Clean. Prod. 379. https://doi.org/10.1016/j.jclepro.2022.134450.

Huang, C., Chui, Y., Gong, M., Chana, F., 2020. Mechanical behaviour of wood compressed in radial direction: Part II. Influence of temperature and moisture content. J. Bioresour. Bioprod. 5, 266–275. https://doi.org/10.1016/j.jobab.2020.10.005.

Huang, D., Li, J., Li, S., Hu, J., Cao, Z., Guo, Y., Ding, Y., Zhu, M., Chen, Y., 2025. Self-densified super-strong wood. J. Bioresour. Bioprod. 10, 199–208. https://doi.org/10.1016/j.jobab.2025.03.001.

Jiang, J., Peng, Y., Ran, Y., Cao, J., 2022. Pseudo lignin formed from hygrothermally treated holocellulose and its effect on fungal degradation. Ind. Crops Prod. 184. https://doi.org/10.1016/j.indcrop.2022.115004.

Kavyashree, S., Krishna, K.P., 2012. Effect of heat treatment on color changes, dimensional stability, and mechanical properties of wood. J. Wood. Chem. Technol. 32, 304–316. https://doi.org/10.1080/02773813.2012.674170.

Laine, K., Rautkari, L., Hughes, M., Kutnar, A., 2012. Reducing the set-recovery of surface densified solid Scots pine wood by hydrothermal post-treatment. Eur. J. Wood Wood Prod. 71, 17–23. https://doi.org/10.1007/s00107-012-0647-2.

Laine, K., Segerholm, K., Wålinder, M., Rautkari, L., Hughes, M., 2016. Wood densification and thermal modification: hardness, set-recovery and micromorphology. Wood Sci. Technol. 50, 883–894. https://doi.org/10.1007/s00226-016-0835-z.

Mi, R., Chen, C., Keplinger, T., Pei, Y., He, S., Liu, D., Li, J., Dai, J., Hitz, E., Yang, B., Burgert, I., Hu, L., 2020. Scalable aesthetic transparent wood for energy efficient buildings. Nat. Commun. 11. https://doi.org/10.1038/s41467-020-17513-w.

Mohareb, A., Sirmah, P., Pétrissans, M., Gérardin, P., 2011. Effect of heat treatment intensity on wood chemical composition and decay durability of Pinus patula. Eur. J. Wood Wood Prod. 70, 519–524. https://doi.org/10.1007/s00107-011-0582-7.

Muzamal, M., Gamstedt, E.K., Rasmuson, A., 2017. Mechanistic study of microstructural deformation and stress in steam-exploded softwood. Wood Sci. Technol. 51, 447–462. https://doi.org/10.1007/s00226-017-0896-7.

Rahiminejad, M., Räber, V., Ghazi Wakili, K., Geyer, C., Zöllig, S., Renfer, C., 2024. Wooden basements; hygrothermal performance analysis using in-field measurements and numerical simulations. Build. Environ. 256. https://doi.org/10.1016/j.buildenv.2024.111475.

Sánchez-Ferrer, A., Engelhardt, M., Richter, K., 2023. Anisotropic wood–water interactions determined by gravimetric vapor sorption experiments. Cellulose 30, 3869–3885. https://doi.org/10.1007/s10570-023-05093-z.

Sun, B., Zhang, Y., Su, Y., Wang, X., Chai, Y., 2022. Effect of vacuum heat treatment on larch earlywood and latewood cell wall properties. Forests 14. https://doi.org/10.3390/f14010043.

Sundqvist, B., Karlsson, O., Westermark, U., 2006. Determination of formic-acid and acetic acid concentrations formed during hydrothermal treatment of birch wood and its relation to colour, strength and hardness. Wood Sci. Technol. 40, 549–561. https://doi.org/10.1007/s00226-006-0071-z.

Sluiter, A., Hames, B., Ruiz, R., Scarlata, C., Sluiter, J., Templeton, D., Crocker, D., 2008. Determination of Structural Carbohydrates and Lignin in Biomass. Laboratory Analytical Procedure. National Renewable Energy Laboratory, Colorado, USA. In: http://www.nrel.gov/biomass/analytical_procedures.html.

Wang, Z., Sun, B., Chai, B., Liu, J., 2022. Study on properties of heat-treated larch tracheid using infrared imaging and nanoindentation test. J. For. Eng. 7, 67–72. https://doi.org/10.13360/j.issn.2096-1359.202112001.

Windeisen, E., Strobel, C., Wegener, G., 2007. Chemical changes during the production of thermo-treated beech wood. Wood Sci. Technol. 41, 523–536. https://doi.org/10.1007/s00226-007-0146-5.

Xia, Y., Dong, H., Semple, K., Huang, J., Zhang, W., Dai, C., 2025. Drying and heat treatment of bamboo: cell collapse and restoration. Constr. Build. Mater. 466. https://doi.org/10.1016/j.conbuildmat.2025.140314.

Xiang, E., Jin, X., Li, J., Huang, R., 2024. Surface physicochemical properties of surface-compressed wood subjected to superheated steam treatment under varying pressures. Constr. Build. Mater. 418. https://doi.org/10.1016/j.conbuildmat.2024.135444.

Yao, Y., Xi, J., Wang, J., Li, W., Shi, J., Yang, Z., Wang, X., 2023. The effects of surface modification by using phytic acid-based hybrid complexes on the interfacial properties of heat-treated wood. Constr. Build. Mater. 403. https://doi.org/10.1016/j.conbuildmat.2023.133118.

Yue, K., Qian, J., Wu, P., Jiao, X., Lu, D., Song, X., 2023. Experimental analysis of thermally-treated Chinese poplar wood with focus on structural application. Ind. Crops Prod. 197. https://doi.org/10.1016/j.indcrop.2023.116612.

Zauer, M., Meissner, F., Plagge, R., Wagenführ, A., 2016. Capillary pore-size distribution and equilibrium moisture content of wood determined by means of pressure plate technique. Holzforschung 70, 137–143. https://doi.org/10.1515/hf-2014-0340.

Zhao, X., Huang, Y., Fu, H., Wang, Y., Wang, Z., Sayed, U., 2021. Deflection test and modal analysis of lightweight timber floors. J. Bioresour. Bioprod. 6, 266–278. https://doi.org/10.1016/j.jobab.2021.03.004.

Zhao, S., Zhang, W., Meng, F., Wei, J., Bao, Y., Li, N., Lin, F., Wang, Z., Bao, M., 2024a. Effect of thermo-mechanical treatment with different initial moisture content on bamboo cell walls. Constr. Build. Mater. 411. https://doi.org/10.1016/j.conbuildmat.2023.134801.

Zhao, X., Zhao, Y., Yu, C., Wang, X., Pan, B., 2024b. Effects of the combination of phenolic-resin impregnation and heat treatment on physical, mechanical and decay resistance of Taxodium hybrid "*Zhongshanshan*" wood. Wood Mater. Sci. Eng. 19, 1091–1100. https://doi.org/10.1080/17480272.2024.2303410.

Zhu, Z., Song, X., Chi, X., Zhao, J., Zhou, Q., Sanchez-Ferrer, A., Tu, D., Cheng, W., 2024a. Characterization of hygrothermal, gas pressure and stress characteristics for poplar wood during unilateral surface densification. Constr. Build. Mater. 438. https://doi.org/10.1016/j.conbuildmat.2024.137099.

Zhu, Z., Tu, D., Chen, Z., Chen, C., Zhou, Q., 2021. Effect of hot pressing modification on surface properties of rubberwood (*Hevea brasiliensis*). Wood Res. 66, 129–139. https://doi.org/10.37763/wr.1336-4561/66.1.129140.

Zhu, Z., Zhou, Q., Cheng, W., Zhao, J., Tu, D., 2024c. Effect of unilateral surface compression technique and heat treatment on industrial application performance of poplar. Ind. Crops Prod. 211, 118287. https://doi.org/10.1016/j.indcrop.2024.118287.

Zhu, Z., Zhou, Q., Cheng, W., Zhao, J., Tu, D., 2024b. Effect of unilateral surface compression technique and heat treatment on industrial application performance of poplar. Ind. Crops Prod. 211. https://doi.org/10.1016/j.indcrop.2024.118287.

Zouari, M., Marrot, L., DeVallance, D.B., 2024. Functional biocarbon-based coatings for wood protection and indoor air depollution. Build. Environ. 261. https://doi.org/10.1016/j.buildenv.2024.111716.